DALTON
FULL PAPER

Dimolybdenum(II) complexes linked by axial cyano bridges to organic and organometallic ligands: syntheses, structures, and characterization †

Wen-Mei Xue, Fritz E. Kühn,* Guofang Zhang, Eberhardt Herdtweck and Gabriele Raudaschl-Sieber

Anorganisch-chemisches Institut der Technischen Universität München, Lichtenbergstraße 4, D-85747 Garching bei München, Germany. E-mail: fritz.kuehn@ch.tum.de

Received 14th June 1999, Accepted 11th October 1999

Reaction of *trans*-[$Mo_2(\mu\text{-}OAc)_2(dppma)_2(NCCH_3)_n][BF_4]_2$ ($n = 0$–2, dppma = bis(diphenylphosphino)methylamine) with a variety of ligands containing a nitrile group leads to axially substituted complexes of formula *trans*-[$Mo_2(\mu\text{-}OAc)_2(dppma)_2(RCN)_2][BF_4]_n$ ($n = 0, 2$), R can be both an organic and an organometallic moiety. The obtained complexes are characterized by ^{1}H-, ^{13}C-, and $^{31}P\{^1H\}$-NMR, IR, Raman, and UV/Vis spectroscopy, elemental analyses and cyclic voltammetry. Four of these complexes are additionally examined by single crystal X-ray analysis. The applied methods show that the axial ligands influence the spectroscopic and crystallographic data of the central moiety only slightly. However, while X-ray crystallography shows the MoMo quadruple bond length not to be significantly influenced by axial ligands, Raman spectroscopy gives a more detailed insight: organic ligands of the type NCR (R = CH_3, *t*-Bu, C_6H_5 *etc.*) in axial positions weaken the MoMo interaction less than organometallic ligands of the type $[NC–M(CO)_5]^-$ (M = Cr, Mo, W) and NCFe$(CO)_2$Cp. UV/Vis examination indicates charge transfer from the organometallic axial ligands to the MoMo moiety.

Introduction

Numerous and varied molecules containing MoMo quadruple bonds are known.[1] However, the number of compounds of the type $[Mo_2(\mu\text{-}OAc)_2(LL)_2]X_2$ where OAc is a bridging acetate ligand and LL is a diphosphine ligand is rather limited for these molecules have been regarded as difficult to handle.[2] Nearly all of the structurally characterized complexes of this type have been described in the last decade.[3] In these molecules the ligands X are in most cases halides, fixed in a position axial to the metal center with rather long metal–halide bond distances.[3c] The compounds are usually synthesized by the reaction of $Mo_2(OAc)_4$ with $(CH_3)_3SiX$ in the presence of diphosphines. Molecules of the type Mo_2X_4(diphosphine)$_2$ can be formed as byproducts or major products, depending on the reaction conditions.[3c,e,f] Closely related to the $[Mo_2(\mu\text{-}OAc)_2(LL)_2]X_2$ complexes are compounds of the type $[Mo_2(\mu\text{-}OAc)_2(LL)_2(S)_n][BF_4]_2$ ($n = 0$–2) where the halide ligands are usually replaced by non coordinating tetrafluoroborates. The axial position in these compounds can be occupied by solvent molecules S; in all cases described to date S = acetonitrile.[3a,b] It should be possible to replace these solvent molecules by other organic and inorganic donor ligands, both by neutral molecules and anions. Recently we reported on the first dirhenium complexes of the type $Re_2(\mu\text{-}O_2CR)_4L_2$, where L is an organometallic ligand which was introduced by the replacement of axial halide ion.[4] These reactions could only be achieved by organometallic anions as new axial ligands. In the present work we extend our examinations to Mo_2 complexes and report on the preparation, structures, and spectroscopic properties of compounds of the type $[Mo_2(\mu\text{-}OAc)_2(LL)_2(L')_2][BF_4]_2$ and $Mo_2(\mu\text{-}OAc)_2(LL)_2(L'')_2$ (L′ and L″ are organic or organometallic ligands). It will be shown that the replacement of the axial solvent molecules enables the introduction of both neutral and anionic ligands and provides an easy access to a much broader variety of axial ligands than the rather limited $(CH_3)_3$SiX/diphosphine route mentioned above.

Experimental

General

All preparations and manipulations were carried out under an oxygen- and water-free argon atmosphere using standard Schlenk techniques. Solvents were distilled over sodium–benzophenone (diethyl ether, hexane), calcium hydride (methylene chloride), methanol (magnesium powder) and P_2O_5 (acetonitrile) and kept over 4 Å (diethyl ether, *n*-hexane and methylene chloride) and 3 Å (acetonitrile, methanol) molecular sieves. Bis(diphenylphosphino)methylamine (dppma) was prepared as described previously.[3d] *cis*-$[Mo_2(\mu\text{-}O_2CCH_3)_2(CH_3CN)_6][BF_4]_2$,[5] Na$[(CO)_5M–CN]$ (M = Cr, Mo, W),[6] Cp$(CO)_2$Fe–CN[7] and *p*-ethynylbenzenonitrile[8] were prepared according to the literature methods. Anhydrous 2,2-dimethylpropanenitrile and benzonitrile were used as received from Aldrich.

Elemental analyses were performed in the Mikroanalytisches Labor of the TU München in Garching (Mr M. Barth). ^{1}H, ^{13}C and $^{31}P\{^1H\}$ NMR were obtained with a Bruker Avance DPX-400 spectrometer. IR spectra were obtained on a Perkin-Elmer FT-IR spectrometer using KBr pellets as IR matrix. Raman spectra were measured by back scattering at room temperature with an S. A. (Riber Jobin Yvon) Model S3000 instrument equipped with a Coherent Innova 301 Kr ion laser (647.1 nm). Electronic absorption spectra were run using a Perkin-Elmer Lambda 2 UV/VIS spectrometer. Cyclic voltammograms were recorded with a computer-controlled D 6734 Lambrecht Potentiostat Galvanostat (HEKA elektronik) in argon-saturated and dried methylene chloride solution with tetrabutylammonium hexafluorophosphate (TBAH, 0.1 M) as supporting electrolyte. The working electrode was platinum and the reference electrode was silver coated with AgCl. Potentials are quoted *vs.* the ferrocene–ferrocenium couple as an internal standard.

---

† *Supplementary data available*: rotatable 3-D crystal structure diagram in CHIME format. See http://www.rsc.org/suppdata/dt/1999/4103/

Preparations

***trans*-[Mo$_2$(μ-O$_2$CCH$_3$)$_2$(μ-dppma)$_2$(CH$_3$CN)$_2$][BF$_4$]$_2$ 1 and *trans*-[Mo$_2$(μ-O$_2$CCH$_3$)$_2$(μ-dppma)$_2$(BF$_4$)$_2$] 2.** 0.23 g (0.32 mmol) of *cis*-[Mo$_2$(μ-O$_2$CCH$_3$)$_2$(CH$_3$CN)$_6$][BF$_4$]$_2$ and 0.27 g (0.67 mmol) of dppma were dissolved in 20 cm^3 of acetonitrile. The purple solution was stirred at room temperature for 4 h and then the solvent was reduced to *ca.* 5 cm^3. Diffusion of diethyl ether through a layer of *n*-hexane into this solution led to red-coloured crystals of **1** suitable for X-ray analysis. Yield: 0.26 g, 83% based on *cis*-[Mo$_2$(μ-O$_2$CCH$_3$)$_2$(CH$_3$CN)$_6$][BF$_4$]$_2$. Drying the solid of **1** at room temperature *in vacuo* (1 mmHg) until the *ν*(C≡N) vibration disappeared from the IR spectrum gave complex **2**. The crystals of **2** for X-ray analysis were obtained by diffusion of diethyl ether into a methylene chloride solution of the compound.

1: Anal. calc. for $C_{58}H_{58}B_2F_8Mo_2N_4O_4P_4$ (1364.5) (%): C, 51.01; H, 4.25; N, 4.10. Found (%): C, 50.47; H, 4.22; N, 3.41. IR (cm^{-1}): 3056m, 2968m, 2934m, 2852m, 2250m (*ν*(C≡N)), 1636w, 1482m, 1436vs, 1190m, 1098vs, 1059vs, 885s, 748s, 698s, 670m, 644m, 526s, 498m, 472m, 429w. ^{1}H NMR (CD$_2$Cl$_2$): *δ* 1.95 (s, 6, CH$_3$CN), 2.09 (s, 6, CH$_3$C), 2.34 (s, 6, CH$_3$N), 7.42–7.72 (m, 40, Ph–H). ^{13}C NMR (CD$_2$Cl$_2$): *δ* 1.9 (*C*H$_3$CN), 23.7 (*C*H$_3$C), 33.9 (CH$_3$N), 119.5 (CN), 129.6, 132.7, 133.4 (Ph–C), 189.1 (CO$_2$). ^{31}P{^{1}H} NMR (CD$_2$Cl$_2$): *δ* 99.7 (s).

2: Anal. calc. for $C_{54}H_{52}B_2F_8Mo_2N_2O_4P_4$ (1281.5) (%): C, 50.57; H, 4.06; N, 2.18. Found (%): C, 50.68; H, 4.21; N, 2.07. IR (cm^{-1}): 3056w, 2938w, 1633w, 1483m, 1436vs, 1184m, 1098vs, 1083vs, 1000m, 962m, 879s, 748s, 695s, 668m, 641m, 527s, 500m, 470m. ^{1}H NMR (CDCl$_3$): *δ* 2.10 (s, 6, CH$_3$C), 2.34 (s, 6, CH$_3$N), 7.49 (m, 40, Ph–H). ^{13}C NMR (CDCl$_3$): *δ* 23.3 (*C*H$_3$C), 34.0 (CH$_3$N), 128.3, 129.0, 131.8, 133.1, 133.3 (Ph–C), 188.0 (CO$_2$). ^{31}P{^{1}H} NMR (CDCl$_3$): *δ* 99.7 (s).

***trans*-[Mo$_2$(μ-O$_2$CCH$_3$)$_2$(μ-dppma)$_2$(NCR)$_2$][BF$_4$]$_2$ (R = C(CH$_3$)$_3$, 3; C$_6$H$_5$, 4; C$_6$H$_4$C≡CH, 5).** To a methylene chloride solution of **1** (0.23 g, 0.32 mmol) was added 0.26 cm^3 (1.28 mmol) of benzonitrile or 0.14 cm^3 (1.28 mmol) of 2,2-dimethylpropanenitrile or 0.41 g (3.2 mmol) of *p*-ethynylbenzenonitrile, respectively. The reaction mixture was then stirred at room temperature for 24 h. After being concentrated to *ca.* 5 cm^3, the solution was layered with a mixture of diethyl ether and *n*-hexane. Red crystals were obtained for each compound. Yield: 0.21 g, 80% for **3**; 0.23 g, 89% for **4** and 0.45 g, 92% for **5** based on **1**.

3: Anal. calc. for $C_{64}H_{70}B_2F_8Mo_2N_4O_4P_4$ (1448.7) (%): C, 53.06; H, 4.87; N, 3.87. Found (%): C, 52.63; H, 4.85; N, 3.69. IR (cm^{-1}): 3052w, 2977w, 2933w, 2251m (*ν*(C≡N)), 1481m, 1435vs, 1123m, 1098vs, 1083vs, 1056vs, 1036m, 881s, 748s, 697s, 526s, 500m, 479m. ^{1}H NMR (CD$_2$Cl$_2$): *δ* 1.34 (s, 18, (CH$_3$)$_3$C), 2.09 (s, 6, CH$_3$C), 2.34 (s, 6, CH$_3$N), 7.48–7.55 (m, 40, Ph–H). ^{13}C NMR (CD$_2$Cl$_2$): *δ* 23.4 (*C*H$_3$CO$_2$), 27.6 ((*C*H$_3$)$_3$C), 30.6 ((CH$_3$)$_3$*C*), 33.5 (CH$_3$N), 128.5 (CN), 129.3, 132.4, 133.0 (Ph–C), 188.7 (CO$_2$). ^{31}P{^{1}H} NMR (CD$_2$Cl$_2$): *δ* 99.7 (s).

4: Anal. calc. for $C_{68}H_{62}B_2F_8Mo_2N_4O_4P_4$ (1488.7) (%): C, 54.90; H, 4.24; N, 3.77. Found (%): C, 54.56; H, 4.03; N, 3.59. IR (cm^{-1}): 3049w, 2934w, 2235m (*ν*(C≡N)), 1619m, 1482m, 1436vs, 1186m, 1124vs, 1083vs, 998m, 882s, 763m, 746s, 698s, 668m, 642m, 525s, 501m, 471m. ^{1}H NMR (CD$_2$Cl$_2$): *δ* 2.26 (s, 6, CH$_3$C), 2.43 (m, 6, CH$_3$N), 7.50–7.73 (m, 50, Ph–H). ^{13}C NMR (CD$_2$Cl$_2$): *δ* 23.0 (*C*H$_3$C), 30.7 (CH$_3$N), 120.4 (CN), 129.6, 132.6, 133.1 (Ph–C), 189.0 (CO$_2$). ^{31}P{^{1}H} NMR (CD$_2$Cl$_2$): *δ* 99.1 (s).

5: Anal. calc. for $C_{72}H_{62}B_2F_8Mo_2N_4O_4P_4$ (1535.4) (%): C, 56.27; H, 4.04; N, 3.65. Found (%): C, 56.38; H, 3.91; N, 3.49. IR (cm^{-1}): 3244s (*ν*(C*C–H*)), 3092w, 3056w, 2939w, 2235s (*ν*(C≡N)), 2106w (*ν*(C≡C)), 1601w, 1438vs, 1403m, 1099vs, 1070vs, 998m, 878s, 850m, 748m, 698m, 668s, 642m, 562m, 524m, 502m, 469m. ^{1}H NMR (CD$_2$Cl$_2$): *δ* 2.20 (s, 6, CH$_3$C), 2.36 (m, 6, CH$_3$N), 3.39 (s, 2, CCH), 7.39–7.67 (m, 48, Ph–H). ^{13}C NMR (CD$_2$Cl$_2$): *δ* 23.7 (*C*H$_3$C), 33.8 (CH$_3$N), 82.0 (CCH), 112.0 (Ph–C), 119.9 (CN), 129.6, 132.4, 133.0, 133.4 (Ph–C), 189.1 (CO$_2$). ^{31}P{^{1}H} NMR (CD$_2$Cl$_2$): *δ* 101.0 (s).

***trans*-[Mo$_2$(μ-O$_2$CCH$_3$)$_2$(μ-dppma)$_2$][NC–M(CO)$_5$]$_2$ (M = Cr, 6; Mo, 7; W, 8).** A solution of **1** (0.14 g, 0.11 mmol) and Na[NC–M(CO)$_5$] (M = Cr, Mo, W, 0.22 mmol) in 10 cm^3 of acetonitrile was stirred at room temperature for 2 h, leading to a red precipitate which was collected and washed with small portions of methanol several times. Yield: 0.14 g, 81% for **6**; 0.08 g, 47% for **7** and 0.16 g, 78% for **8** based on **1**.

6: Anal. calc. for $C_{66}H_{52}Cr_2Mo_2N_4O_{14}P_4$ (1544.9) (%): C, 51.27; H, 3.37; N, 3.62. Found (%): C, 50.92; H, 3.30; N, 3.46. IR (cm^{-1}): 3061w, 2923w, 2101m (*ν*(C≡N)), 2048s, 1972m, 1926vs, 1902vs, 1630w, 1482m, 1434s, 877m, 745m, 696m, 678s, 663s, 642m, 526m, 502m, 470m. ^{1}H NMR (CD$_2$Cl$_2$): *δ* 2.25 (s, 6, CH$_3$C), 2.38 (s, 6, CH$_3$N), 7.23–7.41 (m, 40, Ph–H). ^{13}C NMR (CD$_2$Cl$_2$): *δ* 22.5 (*C*H$_3$C), 32.0 (CH$_3$N), 127.2 (CN), 130.2, 131.1, 131.2, 132.2 (Ph–C), 187.0 (CO$_2$), 215.5 (CO). ^{31}P{^{1}H} NMR (CD$_2$Cl$_2$): *δ* 103.2 (s).

7: Anal. calc. for $C_{66}H_{52}Mo_4N_4O_{14}P_4$ (1632.8) (%): C, 48.51; H, 3.18; N, 3.43. Found (%): C, 48.13; H, 2.97; N, 3.17. IR (cm^{-1}): 3060w, 2931w, 2099m (*ν*(C≡N)), 2055s, 1978m, 1928vs, 1901vs, 1636w, 1483m, 1436vs, 881m, 746m, 694m, 668s, 642m, 608m, 594m, 526m, 499m, 472m. ^{1}H NMR (CD$_2$Cl$_2$): *δ* 2.25 (s, 6, CH$_3$C), 2.63 (s, 6, CH$_3$N), 7.48–7.56 (m, 40, Ph–H). ^{13}C NMR (CD$_2$Cl$_2$): *δ* 24.0 (*C*H$_3$C), 31.0 (*C*H$_3$N), 125.0 (CN), 129.7, 132.0, 133.1, 134.0 (Ph–C), 188.5 (CO$_2$), 194.1, 217.4 (CO). ^{31}P{^{1}H} NMR (CD$_2$Cl$_2$): *δ* 101.2 (s).

8: Anal. calc. for $C_{66}H_{52}Mo_2N_4O_{14}P_4W_2$ (1808.6) (%): C, 43.79; H, 2.88; N, 3.10. Found (%): C, 43.31; H, 2.39; N, 2.92. IR (cm^{-1}): 3061w, 2962w, 2101m (*ν*(C≡N)), 2052s, 1967m, 1918vs, 1896vs, 1653w, 1436s, 882m, 800m, 747m, 693m, 668s, 643m, 598m, 584m, 525m, 499m, 471m. ^{1}H NMR (CD$_2$Cl$_2$): *δ* 2.08 (s, 6, CH$_3$C), 2.19 (s, 6, CH$_3$N), 7.16–7.36 (m, 40, Ph–H). ^{13}C NMR (CD$_2$Cl$_2$): *δ* 24.1 (*C*H$_3$C), 30.1 (*C*H$_3$N), 125.2 (CN), 129.0, 131.8, 133.6 (Ph–C), 189.0 (CO$_2$), 219.1 (CO). ^{31}P{^{1}H} NMR (CD$_2$Cl$_2$): *δ* 101.2 (s).

***trans*-{Mo$_2$(μ-O$_2$CCH$_3$)$_2$(μ-dppma)$_2$[NC–Fe(CO)$_2$Cp]$_2$}[BF$_4$]$_2$ 9.** To a solution of 0.13 g (0.10 mmol) of **1** in methylene chloride was added Cp(CO)$_2$Fe–CN (41 mg, 0.20 mmol) at −40 °C. The solution was allowed to gradually warm up to room temperature after being stirred at −40 °C for 2 h. The solvent was removed *in vacuo* to give the pink-red product, which was washed with diethyl ether. Yield: *ca.* 100% based on **1**. Anal. calc. for $C_{70}H_{62}B_2F_8Fe_2Mo_2N_4O_8P_4$ (1688.4) (%): C, 49.75; H, 3.67; N, 3.32. Found (%): C, 49.29; H, 3.93; N, 3.06. IR (cm^{-1}): 3115w, 3053w, 2923w, 2117m (*ν*(C≡N)), 2056vs, 2008vs, 1616w, 1483m, 1436vs, 1083vs, 878m, 749m, 696m, 641m, 609m, 526m, 499m, 470m. ^{1}H NMR (CD$_2$Cl$_2$): *δ* 2.21 (s, 6, CH$_3$C), 2.37 (s, 6, CH$_3$N), 4.47 (s, 10, Cp), 7.43–7.67 (m, 40, Ph–H). ^{13}C NMR (CD$_2$Cl$_2$): *δ* 23.9 (*C*H$_3$C), 33.9 (CH$_3$N), 85.7 (Cp), 129.7 (CN), 132.7, 133.0 (Ph–C), 189.1 (CO$_2$), 208.7, 224.6 (CO). ^{31}P{^{1}H} NMR (CD$_2$Cl$_2$): *δ* 100.5 (s).

X-Ray crystallography

Preliminary examination and data collection for **1**·4(CH$_3$CN) were carried out on a NONIUS CAD4 four circle diffractometer equipped with a sealed tube; for **2**·2(CH$_2$Cl$_2$) on an imaging plate diffraction system (IPDS; STOE&CIE) equipped with a rotating anode (NONIUS FR591); for **2**·1/2(C$_4$H$_{10}$O, C$_6$H$_{14}$), **4** and **5** on a four-circle diffractometer (NONIUS MACH3) equipped with an area detecting system (NONIUS Kappa-CCD), and a rotating anode (NONIUS FR591). All structures were solved by a combination of Patterson methods

Table 1 Crystallographic data for **1**·4(CH_3CN), **2**·2(CH_2Cl_2), **2**·1/2($C_4H_{10}O$, C_6H_{14}), **4** and **5**

	1·4(CH_3CN)	**2**·2(CH_2Cl_2)	**2**·1/2($C_4H_{10}O$, C_6H_{14})	**4**	**5**
Chemical formula	$C_{66}H_{70}B_2F_8Mo_2N_8O_4P_4$	$C_{112}H_{112}B_4Cl_8F_{16}$-$Mo_4N_4O_8P_8$	$C_{118}H_{128}B_4F_{16}Mo_4$-$N_4O_9P_8$	$C_{68}H_{62}B_2F_8Mo_2$-$N_4O_4P_4$	$C_{72}H_{62}B_2F_8Mo_2N_4O_4P_4$
FW	1528.68	2904.42	2725.01	1488.60	1536.64
Crystal system	Monoclinic	Triclinic	Triclinic	Monoclinic	Monoclinic
Space group	$P2_1/c$	$P\bar{1}$	$P\bar{1}$	$P2_1/n$	$P2_1/n$
a/pm	1257.0(5)	1371.1(1)	1580.37(3)	1371.89(4)	1330.57(3)
b/pm	2413.5(5)	1400.3(1)	1913.09(3)	1619.30(5)	1641.02(3)
c/pm	2296.9(9)	1782.2(2)	2226.22(4)	1544.51(5)	1639.23(4)
α/°		68.73(1)	77.758(1)		
β/°	93.75(2)	77.20(1)	69.838(1)	105.437(1)	103.550(1)
γ/°		89.44(1)	77.453(1)		
$V/10^6$ pm^3	6953(4)	3100.0(5)	6097.9(2)	3307.3(2)	3479.6(1)
Z	4	1	2	2	2
T/K	163	163	143	163	143
ρ_{calcd}/g cm^{-3}	1.460	1.556	1.484	1.495	1.467
μ/mm^{-1}	4.451	0.750	0.588	0.550	0.525
Data collected (h,k,l)	+15, +25, ±27	±16, ±16, ±21	±19, ±23, ±27	±17, ±20, ±19	±17, ±19, ±21
No. of reflections collected	13023	30270	45149	20864	14627
No. of independent reflections	12451	10855	24833	6982	7325
R_{int}	0.0306	0.0276	0.0280	0.0400	0.0306
$R1$[a]	0.0479	0.0542	0.0554	0.0580	0.0420
$wR2$[b]	0.1044	0.1293	0.0877	0.1099	0.0775
GOF[c]	1.157	1.075	1.019	1.052	1.011

[a] $R1 = \Sigma(||F_o| - |F_c||)/\Sigma|F_o|$; [b] $wR2 = [\Sigma w(F_o^2 - F_c^2)^2/\Sigma w(F_o^2)^2]^{\frac{1}{2}}$; [c] $\mathrm{GOF} = [\Sigma w(F_o^2 - F_c^2)^2/(\mathrm{NO} - \mathrm{NV})]^{\frac{1}{2}}$.

and difference-Fourier syntheses. Full-matrix least-squares refinements were carried out by minimizing $\Sigma w(F_o^2 - F_c^2)^2$ with SHELXL-97 weighting scheme and stopped at shift/err <0.001. Data were corrected for Lorentz and polarization effects.[9a] Neutral atom scattering factors for all atoms and anomalous dispersion corrections for the non-hydrogen atoms were taken from the International Tables for Crystallography.[9b] All calculations were performed on a DEC 3000 AXP workstation and an Intel Pentium II PC, with the STRUX-V[9c] system, including the programs PLATON,[9d] SIR92,[9e] and SHELXL-97.[9f] A summary of the crystal and experimental data is reported in Table 1.

CCDC reference number 186/1688.

See http://www.rsc.org/suppdata/dt/1999/4103/ for crystallographic files in .cif format.

Results and discussion

Synthesis

Reaction of the purple *cis*-$[Mo_2(\mu\text{-}OAc)_2(NCCH_3)_6][BF_4]_2$ with a two-fold stoichiometric amount of the diphosphino ligand dppma in acetonitrile at room temperature leads to the pink *trans*-$[Mo_2(\mu\text{-}OAc)_2(dppma)_2(CH_3CN)_2][BF_4]_2$ **1** according to eqn. (1). Drying the compound *in vacuo* (1 mmHg) for several hours caused a gradual removal of the two axial acetonitrile ligands. Finally a compound of the composition *trans*-$[Mo_2(\mu\text{-}OAc)_2(dppma)_2][BF_4]_2$ **2** remains. This behavior explains the difficulties in obtaining a correct elemental analysis for complex **1**. Several related complexes are known, most prominently $[Mo_2(CH_3CN)_{8-10}][BF_4]_4$, which show a similar behavior *in vacuo*.[10]

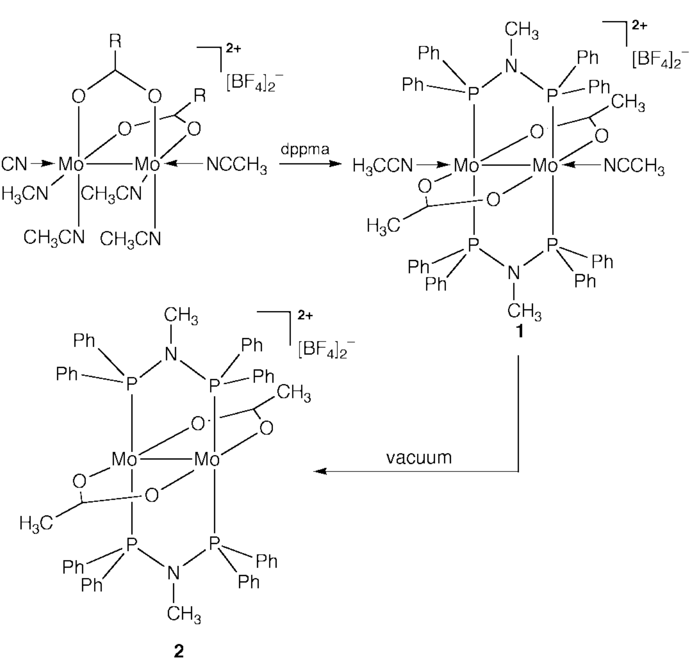

(1)

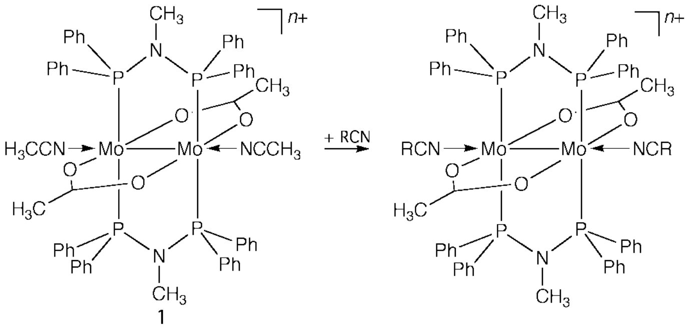

(2)

R	n	Complex
$C(CH_3)_3$	2	**3**
C_6H_5	2	**4**
C_6H_4-C≡CH	2	**5**
$M(CO)_5$	0	M = Cr **6**, Mo **7**, W **8**
$Fe(CO)_2Cp$	2	**9**

Reacting derivative **1** in methylene chloride with an excess of 2,2-dimethylpropanenitrile, benzonitrile, or *p*-ethynylbenzenonitrile leads to complete replacement of the acetonitrile ligand by the nitriles which have been added in excess, especially when the more volatile acetonitrile is partially removed *in vacuo* (eqn. (2)).

The complexes **1**–**5** are soluble in CH_2Cl_2, $CHCl_3$, THF, MeOH, and CH_3CN. In the latter solvent the axial ligands are partially exchanged by solvent molecules. In the solid state the compounds decompose in air within a few days. In solution they are only stable for a few hours when exposed to air or moisture. According to elemental analyses and IR spectroscopy of the brownish precipitates the main decomposition products are molybdenum oxides. Under inert gas atmosphere the compounds are stable for several weeks in solution and for more than one year in the solid state.

Addition of a two-fold stoichiometric amount of Na[NC–$M(CO)_5$] (M = Cr, Mo, W) to an acetonitrile solution of compound **1** at room temperature leads to a precipitate of red derivatives of formula *trans*-$[Mo_2(\mu\text{-}OAc)_2(dppma)_2][(NC\text{–}M(CO)_5)]_2$ **6**–**8** according to eqn. (2). Addition of the neutral ligand NC–$Fe(CO)_2Cp$ at low temperature quantitatively yields the pinkish-red *trans*-$\{Mo_2(\mu\text{-}OAc)_2(dppma)_2[NC\text{–}Fe(CO)_2\text{-}Cp]_2\}[BF_4]_2$ **9**.

While compounds **6**–**8** are only slightly soluble in CH_2Cl_2 and insoluble in all other common organic solvents, derivative **9** has good solubility in CH_2Cl_2, $CHCl_3$ and CH_3CN. Compounds **6**–**9** are more sensitive to air and moisture in solution than derivatives **1**–**5**. In air the complexes **6**–**9** decompose slowly, under an inert gas atmosphere they are stable for months at room temperature.

Molecular structures

The molecular structures of compounds **1**, **2**, **4**, and **5** have been examined by single crystal X-ray crystallography. Two crystallographically independent molecules A and B in the unit cell were found for the compounds **1**·$4(CH_3CN)$, **2**·$2(CH_2Cl_2)$, and **2**·$1/2(C_4H_{10}O, C_6H_{14})$. Both A and B are located on a crystallographic center of inversion in the midpoint of the Mo–Mo bond except **2**·$1/2(C_4H_{10}O, C_6H_{14})$, in which A performs the center of inversion approximately, whereas B resides on pseudo two-fold axes which pass through the colinear C–C bonds of the acetate groups and the midpoint of the Mo–Mo bond.

The dimensions of eight molecules examined were collected and compared in Table 2. Fig. 1 shows an ORTEP representation of compound **1**. The appropriate labeling scheme valid for all eight molecules described in Table 2 is given in Fig. 2. The Mo–Mo bond distances for all examined molecules are in the narrow interval of 211–213 pm. They do not seem to be significantly affected by the axially coordinated nitrile ligands. The Mo–Mo distances in **2**·$2(CH_2Cl_2)$ and **2**·$1/2(C_4H_{10}O, C_6H_{14})$ are nearly identical even though in the first case the axial positions are unoccupied but in the second the counter ions are fixed by a $F_3B\text{–}F\cdots Mo$ interaction in the axial position. Obviously X-ray crystallography is not such a sensitive tool as Raman spectroscopy in this particular case (see below).

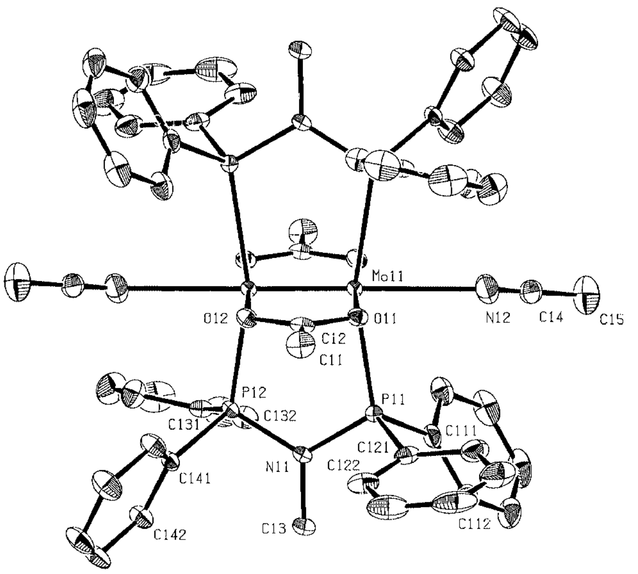

Fig. 1 ORTEP[9d] drawing of the molecular structure of the dicationic part of **1**·$4(CH_3CN)$. Thermal ellipsoids are given at the 50% probability level. Hydrogens omitted are for clarity.

In general, the two bridging acetates and two dppma ligands are arranged *trans* to each other. Two BF_4^- anions or N≡C–R ligands are forced to coordinate to the molybdenum atoms in the axial positions and the Mo–NCR/FBF_3 bond is bent (Fig. 3). Quadruply bonded molybdenum complexes with pairs of bridging dpppa (dpppa = bis(diphenylphosphino)isopropylamine), dppa, dppma and $(O_2CCH_3)^-$ ligands usually have an eclipsed conformation.[1] Both steric (CH_3 instead of H on the bridging nitrogen atom) and electronic (CH_3 shows a stronger inductive effect than H) differences have been considered as being responsible for the nearly two to three times higher

Table 2 Selected interatomic distances (pm), angles (°) and torsion angles (°) for **1**·4(CH_3CN). **2**·2(CH_2Cl_2), **2**·1/2($C_4H_{10}O$, C_6H_{14}), **4** and **5**

		1·4(CH_3CN)	**2**·2(CH_2Cl_2)	**2**·1/2($C_4H_{10}O$, C_6H_{14})[a]		**4**	**5**
Mo–Mo′	A	211.33(9)	211.52(5)	211.51(3)		213.13(4)	213.15(3)
	B	212.95(9)	211.09(6)	211.61(3)			
Mo–P1	A	255.90(14)	257.61(11)	258.17(9)	255.32(9)	257.27(9)	257.03(5)
	B	257.25(14)	257.81(13)	257.05(9)	258.02(9)		
Mo–P2′	A	256.07(14)	258.60(12)	260.28(9)	260.27(9)	257.09(9)	258.39(5)
	B	257.09(14)	259.43(11)	259.18(9)	258.38(9)		
Mo–O1	A	209.7(2)	208.3(3)	208.2(2)	208.7(2)	208.9(2)	209.50(15)
	B	207.9(3)	208.1(3)	209.6(2)	209.5(2)		
Mo–O2′	A	209.5(2)	211.0(3)	210.7(2)	211.3(2)	209.9(2)	210.12(15)
	B	209.6(3)	211.2(3)	210.8(2)	209.9(2)		
Mo–L	A	264.8(4)	250.5(5)	252.0(2)	258.0(3)	258.6(4)	258.2(2)
	B	263.9(4)		252.7(2)	259.2(2)		
P1–N1	A	168.8(3)	169.5(3)	169.4(3)	169.4(3)	169.9(3)	169.4(2)
	B	169.1(3)	170.0(4)	169.2(3)	169.4(3)		
P2–N1	A	168.1(3)	168.6(4)	169.6(3)	170.3(3)	169.3(3)	169.9(2)
	B	168.3(3)	169.0(4)	169.7(3)	169.1(3)		
O1–C2	A	126.2(5)	126.4(4)	127.5(4)	127.6(4)	126.9(4)	127.3(3)
	B	126.6(4)	126.9(4)	127.9(4)	127.7(4)		
O2–C2	A	127.4(4)	127.9(5)	128.4(4)	127.5(4)	128.0(4)	127.6(3)
	B	127.8(4)	126.7(5)	127.3(4)	127.8(4)		
N1–C3	A	147.3(5)	148.4(6)	148.0(5)	148.6(4)	147.8(5)	147.8(3)
	B	147.1(5)	148.9(6)	148.3(4)	148.1(4)		
C2–C1	A	149.5(5)	149.3(6)	147.9(5)	149.4(5)	149.8(5)	150.0(4)
	B	148.1(5)	148.2(7)	149.6(4)	149.2(4)		
Mo′–Mo–L	A	175.56(9)	177.79(15)	177.13(6)	177.56(7)	179.40(9)	178.03(6)
	B	178.06(10)		175.57(6)	175.17(6)		
Mo–L–X	A	144.5(4)	172.5(5)	175.1(2)	166.1(3)	156.8(4)	164.9(2)
	B	162.5(4)		156.7(2)	173.3(2)		
P1–Mo–P2′	A	161.63(4)	160.13(4)	160.60(3)	160.43(3)	161.22(3)	161.61(2)
	B	160.77(4)	160.28(4)	163.62(3)	163.53(3)		
O1–Mo–O2′	A	177.43(10)	177.04(10)	176.72(8)	177.16(8)	177.57(9)	177.42(6)
	B	177.64(9)	177.31(11)	176.95(8)	176.60(8)		
P1–N1–P2	A	117.72(16)	117.9(2)	118.62(16)	116.81(16)	117.58(17)	117.85(11)
	B	118.31(16)	118.3(2)	117.10(16)	118.38(16)		
O1–C2–O2	A	121.0(3)	121.7(4)	121.1(3)	121.4(3)	121.1(3)	121.6(2)
	B	121.1(3)	121.1(3)	121.2(3)	121.5(3)		
P1–Mo–Mo′–P2	A	−7.23(4)	−11.19(4)	−9.02(3)	10.32(3)	−8.80(3)	−7.34(2)
	B	−10.14(4)	−10.00(4)	13.22(3)	10.47(3)		
O1–Mo–Mo′–O2	A	−0.26(10)	−0.67(11)	0.77(8)	1.29(9)	−0.08(9)	0.32(7)
	B	−0.18(9)	−0.12(19)	3.98(9)	3.72(8)		

[a] The bond distances and angles given in column 6 are caused by loss of crystallographic symmetry.

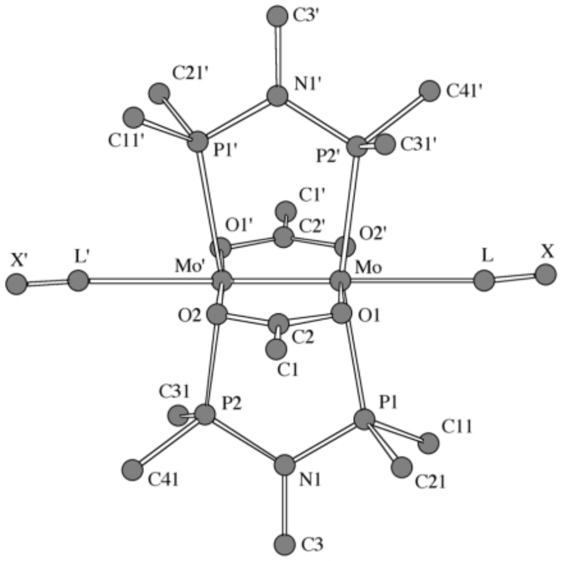

Fig. 2 Schematic drawing with the appropriate labeling scheme for all eight molecules.

torsion angles P–Mo–Mo–P of the dppma complexes compared to those observed in dppa derivatives (mean value 5.2°).[3d] However, the torsion angles are very similar in the case of compound **1** and its dppa congener, in the latter case the P–Mo–Mo–P angle is 9.75(8) and 10.80(0)°, respectively, for the two independent molecules within the unit cell.[3g]

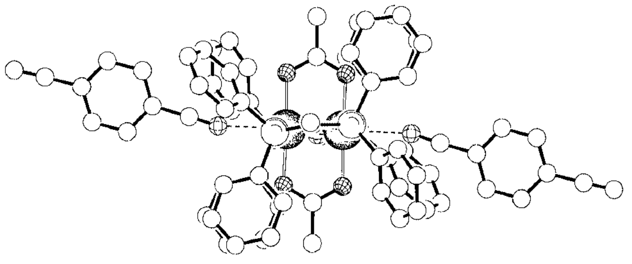

Fig. 3 PLATON[9d] drawing of the molecular structure of the dicationic part of **5**, illustrating the bent bonding of the axial ligands.

The Mo–F/N bonds are comparatively long, indicating only very weak Mo–F/N interactions. However, the Mo–F/N distances are shorter than expected from the sum of the van der Waals radii (Mo–F: 374 pm; Mo–N: 382 pm) but longer than the sum of the covalent radii (Mo–F: 211 pm; Mo–N: 215 pm).[9d]

Spectroscopy

The ^{13}C NMR resonances of the bridging nitrile carbons are listed in Table 3, the data for free ligands are also given for comparison. The signals appear in the region $\delta(^{13}C) = 119.5–128.5$ for **1** and **3**–**5**, each of them is shifted to lower field

Table 3 Selected spectroscopic data of compounds **1**–**9** and pure ligands

Compound	Axial ligand	ν(C≡N)/cm^{-1}	ν(C≡O)/cm^{-1}	$\delta(^{13}C)$CN/ppm	ν(MoMo)/cm^{-1}	$\lambda_{ab/max}$ (ε)/ nm (M^{-1} cm^{-1})
1	NCCH$_3$	2250	—	119.5	361	513 (1740)[a]
CH$_3$CN	—	2250	—	116.3	—	
2	FBF$_3^-$	—	—	—	375	514 (3110)[a]
3	*t*-BuCN	2251	—	128.5	357	514 (1130)[a]
t-BuCN	—	2250	—	125.9	—	
4	NCPh	2235	—	120.4	360	514 (1220)[a]
PhCN	—	2230	—	118.8	—	
5	NCC$_6$H$_4$CCH	2235	—	119.9	360	513 (3030)[a]
HCCC$_6$H$_4$CN	—	2228	—	118.2	—	
6	[NC–Cr(CO)$_5$]$^-$	2101	2048 1972 1926 1902	127.2	334	546 (2120)[a]
[NC–Cr(CO)$_5$]$^-$	—	2111	2051 1996 1942 1919 1830	153.8	—	338 (2230)[b]
7	[NC–Mo(CO)$_5$]$^-$	2099	2055 1978 1928 1901	125.0	337	546 (1043)[a]
[NC–Mo(CO)$_5$]$^-$	—	2106	2058 1986 1935 1909 1831	149.2	—	355 (2980)[b]
8	[NC–W(CO)$_5$]$^-$	2101	2052 1967 1918 1896	125.2	334	546 (1050)[a]
[NC–W(CO)$_5$]$^-$	—	2113	2056 1983 1934 1904 1815	140.0	—	359 (2490)[b]
9	[NC–Fe(CO)$_2$Cp	2117	2056 2008	126.3	337	broad[a]
NC–Fe(CO)$_2$Cp	—	2117	2057 2007	125.9	—	347 (1370)[a]

[a] Measured in CH$_2$Cl$_2$. [b] Measured in MeOH.

by *ca.* 2–3 ppm in comparison to the free ligands. These slight shift changes reflect the weak bonding interactions between nitrile ligands and the MoMo core. For the same reason, the IR vibrational frequencies of C≡N in **1** and **3**–**5** are nearly unchanged compared to the free ligands (Table 3). The FAB mass spectra show only signals for ions lacking the axial ligands. However, the existence of an interaction between the MoMo core and the nitriles in complexes **1** and **3**–**5** is clearly expressed by the reduction in the Raman active ν(MoMo) mode from 375 cm^{-1} in **2** to 357–361 cm^{-1} in **1** and **3**–**5**. The MoMo interaction in the case of the nitrile free complex **2** is clearly stronger than in the cases of the nitrile derivatives **1** and **3**–**5**.

Although no significant difference of the C≡N vibrational frequencies in **6**–**8** compared to their precursor **1** can be observed in the IR spectra, a strong chemical shift difference can be seen in the signal corresponding to the carbon atom of the bridging cyano group in the ^{13}C NMR. This signal is shifted upfield *ca.* 15–25 ppm depending on the central metal of the axial ligand. Interestingly, the chemical shifts of the C≡N carbon atoms are very similar in compounds **6**–**8**. This observation is in remarkable contrast to the Cr, Mo, W precursor molecules and has been also stated for the complexes Re$_2$(μ-O$_2$CCMe$_3$)$_4$[NCM(CO)$_5$]$_2$ (M = Cr, Mo, W).[4] In the case of compound **9**, with its neutral Fe containing ligand, the $\delta(^{13}C)$ of the nitrile carbon atom and the ν(C≡N) and ν(C≡O) IR vibrations remain virtually unchanged upon complexation (see Table 3). However, the ν(C≡O) vibrations of derivatives **6**–**8** are shifted to higher energies in comparison to the starting materials. This implies a decrease in the back-bonding capability to the π* CO ligand orbital from the M (Cr, Mo, W) center because part of the electron density at the M centers is shifted towards the MoMo core *via* the NC-unit.

The strong Raman bands centered at 334, 337, 334 and 337 cm^{-1} for **6**–**9**, respectively, can be unambiguously assigned to stretching frequencies of the quadruple bond between the Mo atoms, which are shifted to lower energies by *ca.* 40 cm^{-1} relative to **2**. This red shift suggests that coupling occurs between the Mo–Mo stretching mode and the Mo–N≡C stretching modes. It is also in accord with the occurrence of a less pronounced MoMo→N≡CR π back-bonding than in the derivatives **1** and **3**–**5** which contain organic axial ligands. The MoMo interaction in complexes **6**–**9** is therefore somewhat weaker than in the derivatives **1** and **3**–**5**. However, a clear dependence of the MoMo bond strength on the ligand metal atom in the group Cr, Mo, W—as it has been observed for the above mentioned Re$^{II}_2$ complexes[4]—cannot be seen.

The weakly bonded organic axial nitriles in compounds **1** and **3**–**5** have no measurable effect on their electronic absorption spectra, all of them show the $\delta_{xy}\rightarrow\delta_{xy}^*$ transition at the same energy (514 nm) although changes in intensity occur (Table 3). The energy of this transition is comparable to other complexes containing both *trans* acetate and phosphine bridges.[3]

The electrochemical properties of complexes **1**–**4** have been investigated by cyclic voltammetry in 0.1 M TBAH–CH$_2$Cl$_2$ and the results are summarized in Table 4. The overall electro-

Table 4 Cyclovoltammetric data[a] of complexes **1**–**4**

Complex	Oxidation process	Reduction process			
1	+1.23(ir)	−1.33(100)	−1.62(90)	−1.90(qr, 50)	−2.18(ir)
2	+1.27(ir)	−1.23(90)	−1.61(70)	−1.87(ir)	−2.13(ir)
3	+1.31(ir)	−1.14(70)	−1.48(90)	−1.74(qr, 80)	−2.03(ir)
4	+1.30(ir)	−1.20(90)	−1.54(90)	−1.83(ir)	−2.09(ir)

[a] Cyclic voltammograms were recorded in 0.1 M TBAH–CH_2Cl_2 at a scan rate of 200 mV s^{-1}. Potentials are in V *vs.* the ferrocene–ferrocenium couple, Fc–Fe^+; error is ±0.2 V; peak–peak separations Δ*E*p for reversible and quasi-reversible couples are given in parentheses.

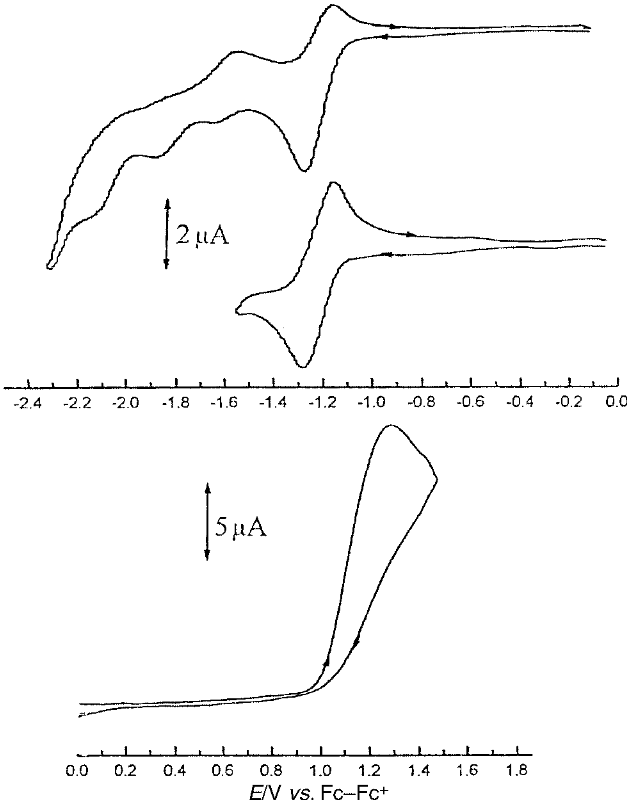

Fig. 4 Cyclic voltammogram of *trans*-$[Mo_2(\mu\text{-}O_2CCH_3)_2(\mu\text{-dppma})_2(CH_3CN)_2][BF_4]_2$ **1** in 0.1 M TBAH–CH_2Cl_2. Scan rate is 200 mV s^{-1}; potentials are *vs.* Fc–Fc^+.

chemical behavior of these derivatives is quite complex. The general polarographic behavior of them is similar. An example is given in Fig. 4. All derivatives display an irreversible oxidation in the potential range 1.23 to 1.31 V *vs.* Fc–Fc^+, which is tentatively assigned to the oxidation of the dppma ligand. This oxidation process is shifted to more positive potential relative to the free ligand (*E*(p,a) = +0.85 V), indicating a metal–ligand interaction which leads to an electron-withdrawing effect on the dppma ligand. However, it cannot be excluded that the irreversible oxidation is due to a $[Mo_2]^{5+/4+}$ process. The cyclic voltammogram of $Mo_2(O_2CCH_3)_4$ in MeOH reveals a metal-based one-electron quasi-reversible oxidation with $E_{1/2}$ = +0.24 V *vs.* Ag–AgCl, no reduction process being observed.[11] In the cases examined here, four quasi-reversible or irreversible reductions have been detected: the first in the range of −1.14 to −1.33 V, the second in −1.48 to −1.62 V, the third in −1.74 to −1.90 V, and the fourth in −2.03 to −2.16 V. By comparison to the electrochemical behavior of mono- and bi-nuclear molybdenum[12] and dimolybdenum thioxanthate complexes,[13] the first reduction is considered to be metal centered. As shown in Fig. 4, the first reduction couple is quasi-reversible when the potential sweep is extended to −2.0 V; i_{pa}/i_{pc} approaches a value of unity when the potential range scanned only covers the first reduction, suggesting a reversible process.

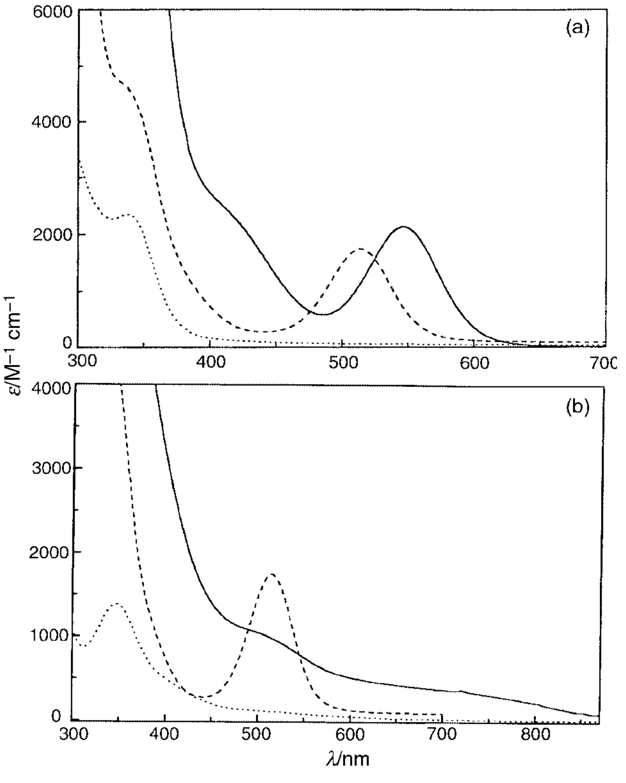

Fig. 5 Comparison of the electronic absorption spectra in CH_2Cl_2 (unless otherwise stated): (a) **6** (——), **1** (----) and $Na[NC\text{–}Cr(CO)_5]$ (·····, MeOH); (b) **9** (——), **1** (----) and $[NC\text{–}Fe(CO)_2Cp]$ (·····).

The UV/Vis spectroscopy data for the complexes **6**–**9** together with their organometallic axial ligands are listed in Table 3. Fig. 5 presents a comparison between the products and their precursors. Each of the derivatives **6**–**8** contains a single broad peak centered at 546 nm which is lower in energy than both of the absorptions from **1** and $[NCM(CO)_5]^-$ (M = Cr, Mo, W), and it is thus tentatively assigned as a MM′CT transition from M^0 to $Mo^{II}Mo^{II}$. It is surprising to observe that this band in **6**–**8** is located at the same energy, despite the different absorption coefficients. After the coordination of the $Cp(CO)_2Fe\text{–}CN$ ligand to the Mo_2 moiety in compound **9**, the electronic spectrum alters significantly, with the appearance of a shoulder extending from 450 to 850 nm. This band can, in principle, be attributed to a charge transfer from the donor moiety, $Cp(CO)_2Fe\text{–}CN$, to the acceptor, $[Mo_2(\mu\text{-}O_2CCH_3)_2(\mu\text{-dppma})_2]^{2+}$.

Conclusions

Molecules of the type *trans*-$[Mo_2(\mu\text{-OAc})_2(dppma)_2][BF_4]_2$ can be easily substituted in the axial positions. A variety of ligands bearing nitrile functionalities can therefore be utilized. Both organic and organometallic, neutral and anionic ligands can be applied to form room temperature stable complexes which are easily accessible in good yields. The axial ligands act as electron donors. The MoMo interaction is therefore slightly weakened, dependent on the donor capabilities of the axial ligands, but the overall influence on the MoMo moiety and the equatorial ligands is comparatively weak in all the cases examined. Raman spectroscopy proves to be the most sensitive tool to establish the influence of the axial ligands on the metal–metal interaction. Due to the very easy and straightforward synthesis of these complexes, ligands which contain more than one nitrile function could be introduced in the axial positions. By this method long chain molecules or two- and three-dimensional networks could be synthesized. Complexes of those types might have interesting properties as materials for nonlinear optics and as electron conductors. Work in this direction is currently under way in our laboratory and will be reported elsewhere.

Acknowledgements

W.-M. X. thanks the Alexander von Humboldt Foundation for a postdoctoral fellowship, G. Z. the Katholischer Akademischer Ausländer-Dienst for a stipend. Professor W. A. Herrmann is acknowledged for generous support.

References

1 F. A. Cotton and R. A. Walton, *Multiple Bonds between Metal Atoms*, 2nd edn., Oxford University Press, London, 1993 and references cited therein.

2 M. Bakir and R. A. Walton, *Polyhedron*, 1988, **7**, 1279.

3 (*a*) L. J. Farrugia, A. McVitie and R. D. Peacock, *Inorg. Chem.*, 1988, **27**, 1257; (*b*) F. A. Cotton, J. Eglin and K. J. Wiesinger, *Inorg. Chim. Acta*, 1992, **195**, 11; (*c*) D. I. Arnold, F. A. Cotton and F. E. Kühn, *Inorg. Chem.*, 1996, **35**, 4733; (*d*) F. A. Cotton, F. E. Kühn and A. Yokochi, *Inorg. Chim. Acta*, 1996, **252**, 251; (*e*) Y. Y. Wu, J. D. Chen, L. S. Liou and J. C. Wang, *Inorg. Chim. Acta*, 1997, **258**, 193; (*f*) D. I. Arnold, F. A. Cotton and F. E. Kühn, *Inorg. Chem.*, 1996, **35**, 5764; (*g*) F. A. Cotton and F. E. Kühn, *Inorg. Chim. Acta*, 1996, **252**, 257.

4 F. E. Kühn, I. S. Gonçalves, A. D. Lopes, J. P. Lopes, C. C. Romão, W. Wachter, J. Mink, L. Hajba, J. A. Parola, F. Pina and J. Sotomayor, *Eur. J. Inorg. Chem.*, 1999, 295.

5 (*a*) F. A. Cotton and K. Wiesinger, *Inorg. Chem.*, 1991, **30**, 871; (*b*) F. A. Cotton and K. Wiesinger, *Inorg. Synth.*, 1992, **29**, 134; (*c*) F. A. Cotton and F. E. Kühn, *J. Am. Chem. Soc.*, 1996, **118**, 5826; (*d*) F. A. Cotton, C. A. Murillo, L. Daniels and X. Wang, *Polyhedron*, 1998, **17**, 2781; (*e*) G. Pimblett, C. D. Garner and W. Clegg, *J. Chem. Soc., Dalton Trans.*, 1986, 1257.

6 (*a*) R. B. King, *Inorg. Chem.*, 1967, **6**, 25; (*b*) J. K. Ruff, *Inorg. Chem.*, 1968, **7**, 1821.

7 P. M. Treichel and D. C. Molzahn, *Synth. React. Inorg. Met.-Org. Chem.*, 1979, **9**, 21.

8 S. Takahashi, Y. Kuroyama, K. Sonogashira and N. Hagihara, *Synthesis*, 1980, 627.

9 (*a*) Z. Otwinowski and W. Minor, *Processing of X-Ray Diffraction Data Collected in Oscillation Mode*, *Methods in Enzymology*, ed. W. C. Carter and R. M. Sweet, Jr., Academic Press, USA, 1996, 276; (*b*) *International Tables for Crystallography*, Vol. C, Tables 6.1.1.4 (pp. 500–502), 4.2.6.8 (pp. 219–222) and 4.2.4.2 (pp. 193–199), Ed. A. J. C. Wilson, Kluwer Academic Publishers, Dordrecht, 1992; (*c*) G. Artus, W. Scherer, T. Priermeier and E. Herdtweck, 'STRUX-V', A Program System to Handle X-Ray Data, TU München, 1997; (*d*) A. L. Spek, PLATON, A Multipurpose Crystallographic Tool, Utrecht University, 1999; (*e*) A. Altomare, G. Cascarano, C. Giacovazzo, A. Guagliardi, M. C. Burla, G. Polidori and M. Camalli, SIR92, *J. Appl. Cryst.*, 1994, **27**, 435; (*f*) G. M. Sheldrick, SHELXL-97, University of Göttingen, 1998.

10 (*a*) J. M. Mayer and E. H. Abbott, *Inorg. Chem.*, 1983, **22**, 2774; (*b*) F. A. Cotton and K. J. Wiesinger, *Inorg. Chem.*, 1991, **30**, 871.

11 A. Carvill, P. Higgins, M. McCann, H. Ryan and A. Shiels, *J. Chem. Soc., Dalton Trans.*, 1989, 2435.

12 A. Das, J. C. Jeffery, J. P. Maher, J. A. McCleverty, E. Schatz, M. D. Ward and G. Wollermann, *Inorg. Chem.*, 1993, **32**, 2145.

13 P. Vella and J. Zubieta, *J. Inorg. Nucl. Chem.*, 1978, **40**, 477.

Paper 9/04742E